

OCURRENCE OF COPPER FILMS IN BASALT FROM THE SERRA GERAL FORMATION, PARANÁ BASIN, BRAZIL

KAZUE TAZAKI*, W.S. FYFE*, KOICHI TAZAKI**, J. BISCHOFF*** and B.R. ROCHA***

ABSTRACT The distribution of trace copper in normal basalt from the Serra Geral Formation, Paraná Basin, Brazil, has been studied using EPMA, SEM with EDX, TEM, and SIMS methods. Relatively fresh basalts show no unique copper phases, and copper was not detected in pyroxene (iron-rich augite) and plagioclase by micro techniques. Copper-rich film are found in altered glassy basalts. Smectite clay, an unidentified Fe-Cu mineral, some Fe-Ti oxides also occur and contain appreciable copper. The copper content for 130 core samples of basalt varies between 150-200 ppm. It seems to exist a positive correlation between electrical conductivity and copper content of basalts. Patterns of electrical conductivity over large areas could be of use in identifying zones of low temperature hydrothermal alteration and in the study of fluid circulation during cooling.

RESUMO OCORRÊNCIA DE FILMES DE COBRE EM BASALTOS DA FORMAÇÃO SERRA GERAL, BACIA DO PARANÁ, BRASIL Alguns basaltos da Formação Serra Geral, Bacia do Paraná, apresentam alta condutividade elétrica relacionada à presença de cobre, embora a quantidade do metal presente não exceda ao normalmente esperado em rochas dessa composição. Amostras de basalto foram estudadas com técnicas de microscopia eletrônica e espectrometria de massa, mostrando a presença de esmectita cuprífera e filmes de cobre em material vítreo alterado. O cobre ocorre também em óxidos de Fe-Ti bem como associado ao Fe em mineral não identificado. O cobre é móvel durante as fases de alteração hidrotermal de baixa temperatura que afetam o basalto. Técnicas de condutividade elétrica podem, portanto, ser utilizadas no estudo do padrão de circulação dos fluidos hidrotermais durante o esfriamento das lavas basálticas.

INTRODUCTION Basalts normally contain about 100 ppm copper. If sulphide minerals occur, these normally carry some copper (e.g. in pyrrhotite) but copper is not concentrated in magnetite. All these primary phases will produce only normal electrical conductivity.

In this study, the distribution of copper in basalt alteration phases is described and correlated with electrical conductivity. High electrical conductivity (by at least two orders of magnitude) does not appear to depend on the bulk copper content but rather depends on the redistribution of copper during low temperature alteration.

The basalt samples studied were collected from drill core in the Serra Geral Formation Paraná Basin, Brazil (borehole 1TP3-SC (Três Pinheiros), coordinates 26°47' 04.1"S, 51°28'32.5"W. The Serra Geral Formation is a volcanic sequence of tholeiitic basalts extracted by fissure eruption. Ages range from late Jurassic to early Cretaceous, typical of the Paraná basalts (Petri & Fúlfaro 1983).

Petrographic observations show augitic pyroxene, plagioclase, and magnetite. A glassy phase is common while calcite and quartz appear in small amounts. Magnetite forms cubes as seen in reflected light while glasses are partially

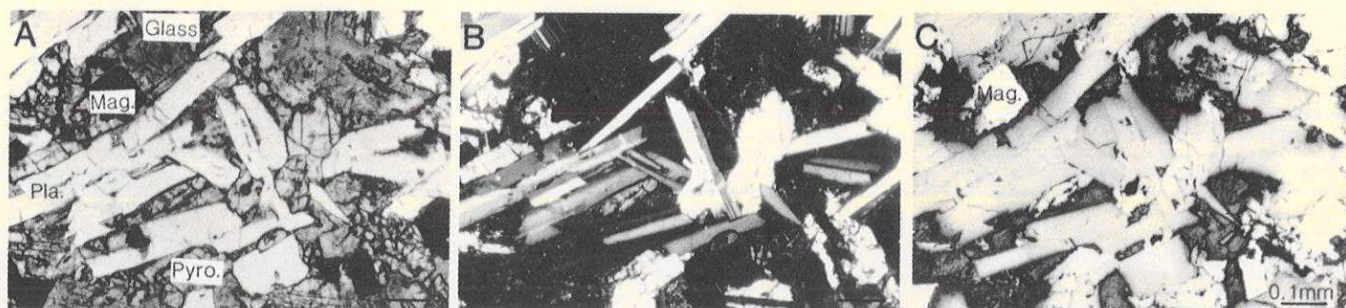


Photo 1 – Optical micrographs showing common minerals in basalts – A: open nichol; B: crossed nichol; C: reflected image. The scale in A and B are the same scale as C

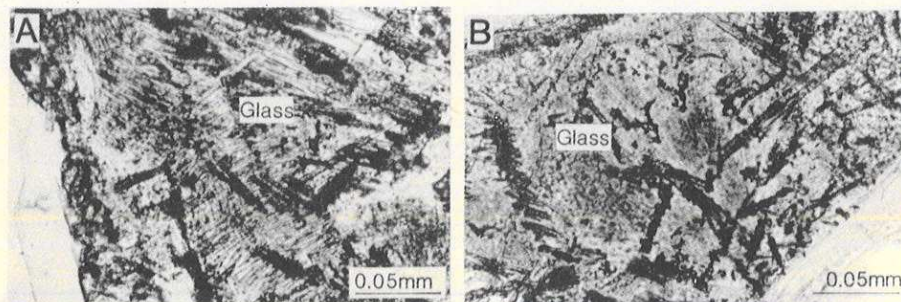


Photo 2 – Optical micrographs showing unaltered glass with devitrification texture (A) and partially altered glass forming smectite (B)

* Department of Geology, The University of Western Ontario, London, Ontario, Canada N6A 5B7

** College of General Education, Ehime University, Matsuyama, Ehime, Japan 790

*** Universidade Federal do Pará, Campus Universitário do Guamá, Centro de Geociências, Caixa Postal 1611, CEP 66000, Belém, Pará, Brasil

devitrified and show alteration to smectite clays with some secondary iron oxides (Photos 1 and 2).

MATERIALS AND METHODS Partially altered materials were separated by hydraulic elutriation methods. Grains, < 2mm, were collected for X-ray powder diffraction (XRD) and transmission electron microscopy (TEM). Grains were also handpicked from bulk samples for scanning electron microscopy and energy dispersive X-ray analysis (SEM-EDX). While no copper-bearing phases were observed by bulk XRD, the electron microscope techniques and secondary ion mass spectrometry (SIMS) provided evidence on the location of copper.

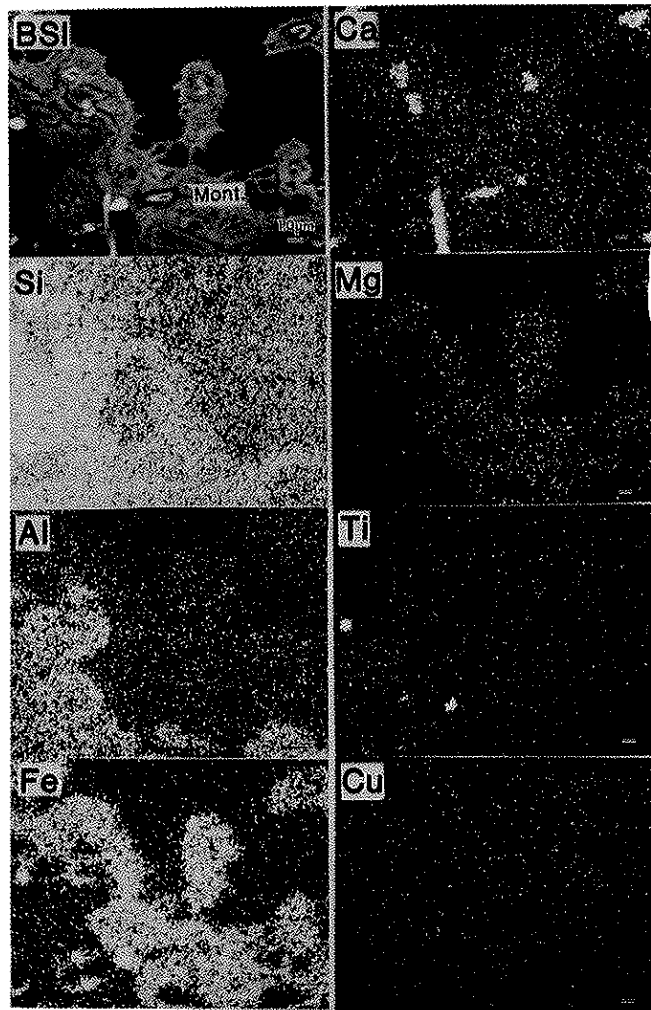


Photo 3 – Back scattered electron image (BSI) and the X-ray images of Si, Al, Fe, Ca, Mg, Ti, and Cu contents of the smectite in the altered glass region. All eight of photographs have the same scale as BSI. Element of a content map shows at the left corner

Electron microscopes SEM was carried out with a JEOL 100C-ASID equipped with EDX and an ISI DC-130 research instrument with an acceleration voltage of 20-30 kV. TEM studies used a JEM 100C instrument with a 100 kV acceleration voltage. Bulk samples were mounted on brass stubs or plated and gold coated for SEM. Powder samples, < 2µm for TEM, were prepared by water suspension methods.

In the EDX results presence of Cu is attributed to characteristic X-ray emission at 8.047 KeV (Cu Kα) that has no contribution of other elements to this peak. Mn-standard sample has been used for procedures of spectral analysis and calibration. Intensity of each element indicates total counts

Table 1 – X-ray fluorescence analysis of the whole rock sample of basalt

Major	%	Trace	ppm
SiO ₂	54.46	Pb	16
TiO ₂	1.76	Zn	94
Al ₂ O ₃	12.07	Cu	118
Fe ₂ O ₃	13.94	Ni	35
MnO	0.22	Co	49
MgO	3.65	Cr	34
CaO	7.69	V	455
K ₂ O	1.60		
P ₂ O ₅	0.24		
Na ₂ O	2.34		
LOI	1.20		
Total	99.18		

LOI: Loss on ignition at 1,000°C

for 100 seconds analytical time showing relative values. Full scale (counts per second) for each EDX spectrum indicates in the left corner of a spectrum that is due to the magnification and probe size. The probe size of 250 Å, the probe current of 8×10^{-11} A, and the magnification from 5,000 to 30,000 have been used in magnifying the display of SEM with EDX.

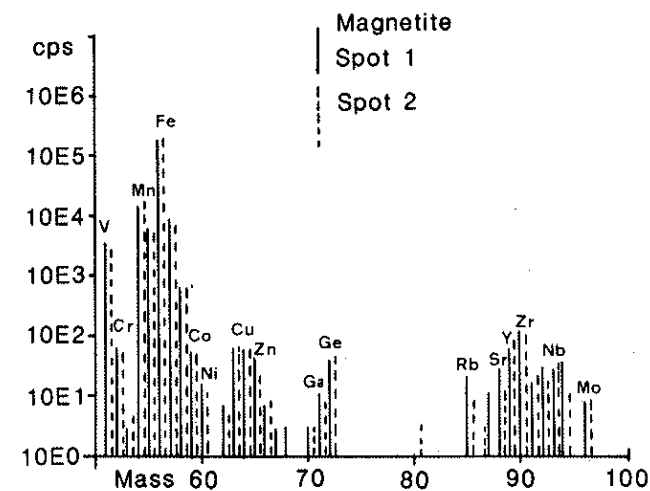
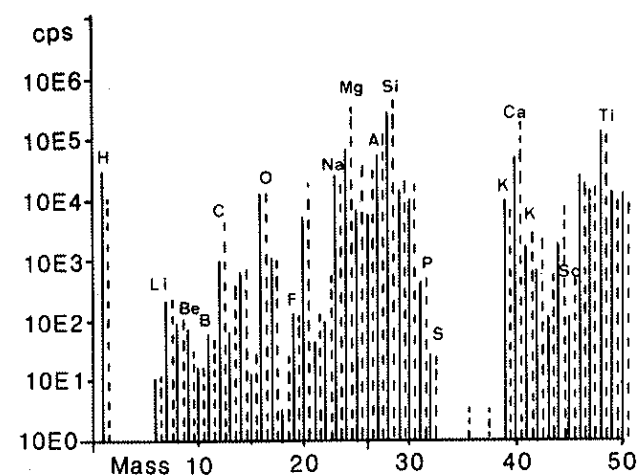


Figure 1 – Secondary ion mass spectra of magnetite crystals. Both spots 1 and 2 show high Ti and Fe contents with trace Cu content. Each element indicates at the top of the bar

X-ray powder diffraction (XRD) XRD was carried out with a Rigaku X-ray diffractometer system, geigerflex CN 2029 D/MAX-1A under the Cu K α radiation, Ni-filter and acc. 30 kV, 20 mA. The < 2 μ m size fraction was oriented on the glass slides with water. Glycerine treatment was used for identification of 14 Å minerals.

X-ray fluorescence analysis (XRF) XRF was carried out with Philip 1450 automatic sequential spectrometer. Major elements and trace elements in the whole rock were calibrated by 16 international standards. The pressed powder pellets were prepared for trace elements.

Secondary ion mass spectrometry (SIMS) SIMS analyses were conducted with a Cameca IMS-3F secondary ion mass spectrometer using $^{16}\text{O}^-$ primary beam. The polished thin sections were analyzed with diameter of approximately 100 μ m, 12.5 KeV primary acc. vol. and +4.5 KeV secondary acc. vol. A mass filtered O^- primary beam produced the positive secondary ion spectrum. SIMS provided evidence on the location of copper of mass numbers 63 and 65.

Electron microprobe analysis (EPMA) Electron probe micro-analysis was made using a Japan Electron Optics Laboratory Co. electron probe X-ray microanalyzer, JEOL 5A at a take-off angle of 40°, with an accelerating voltage of 16 kV and with 2 μ m beam diameter. A natural pyroxene

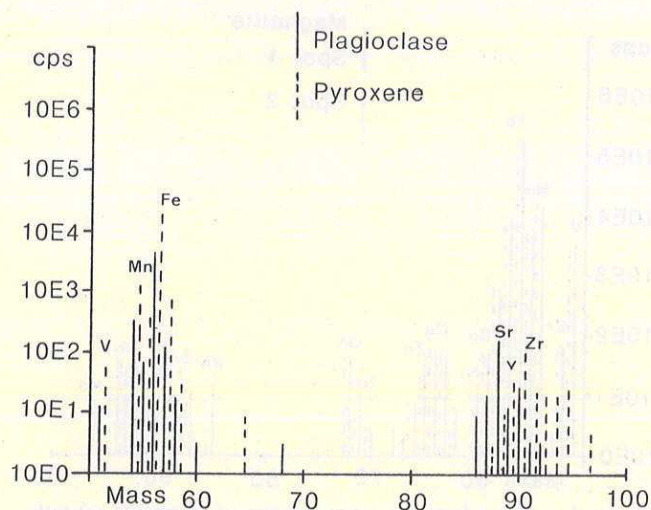
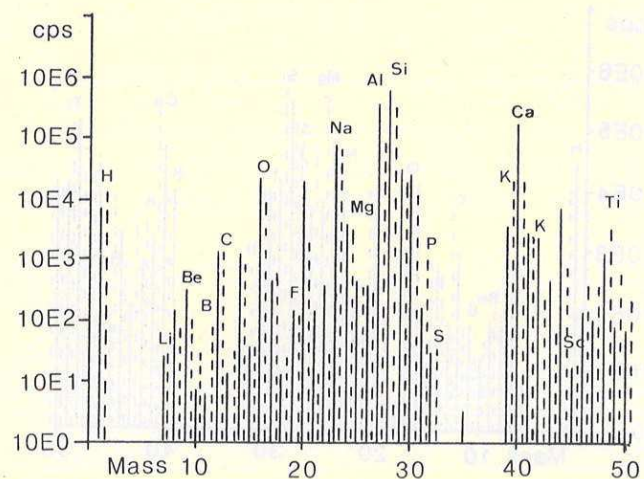


Figure 2 – Secondary ion mass spectra of plagioclase and pyroxene crystals showing no Cu content

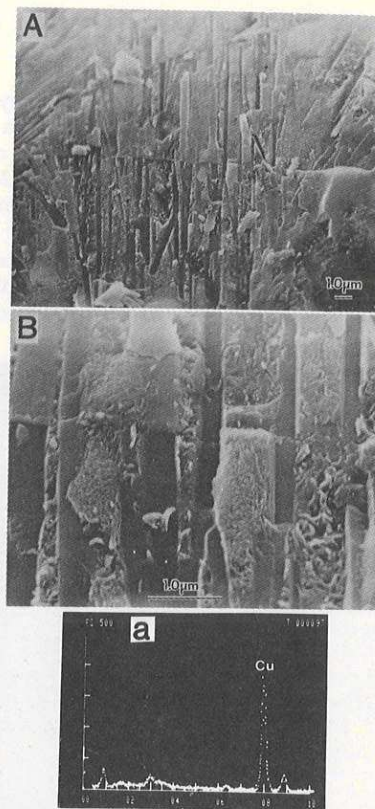


Photo 4 – Scanning electron micrograph of partially altered glass with devitrification texture (A). Area analysis shows an almost pure Cu signal (a). B: higher magnification of devitrification texture of A. The ordinate indicates C.P.S. and the abscissa indicates energy of KeV in all EDX spectra

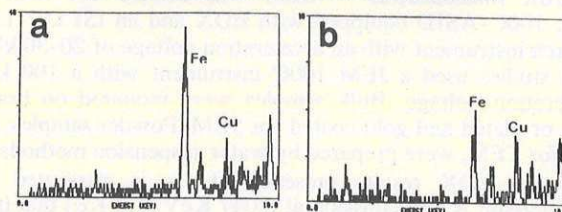
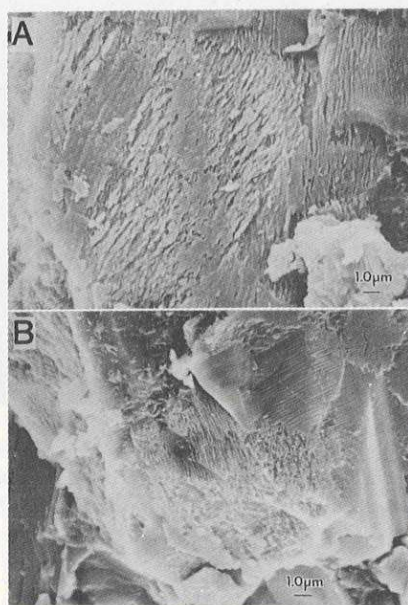


Photo 5 – Scanning electron micrographs of the scaly materials (A and B) and their EDX (a and b) showing Fe and Cu signals

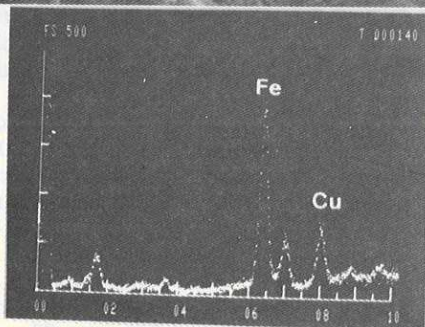
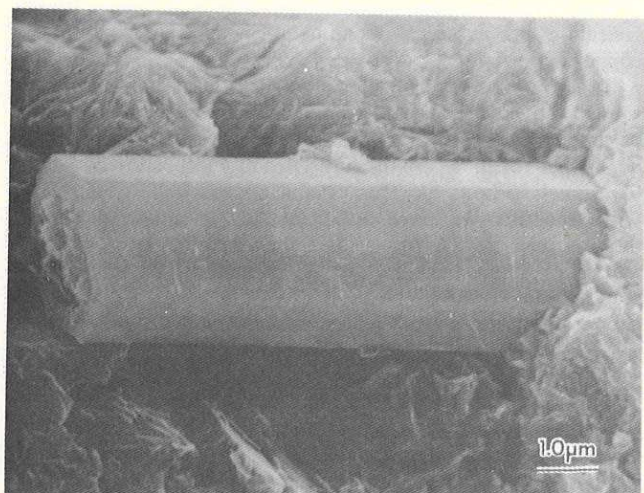


Photo 6 – Scanning electron micrograph of an unidentified hexagonal prism mineral showing Fe and C signals

standard was used for major element analysis. Detection limit for Cu is about 0.03% for this method.

RESULTS Mineralogical and elemental composition
XRD examination of the < 2µm size fraction showed dolomite, calcite, quartz, albite, and small peaks for ilmenite, hematite, and magnetite. No copper phases were distinguished. The presence of smectite was recognized after glycerine treatment, with the separate characteristic peak for smectite (18.0 Å) derived from 14.3 Å peak.

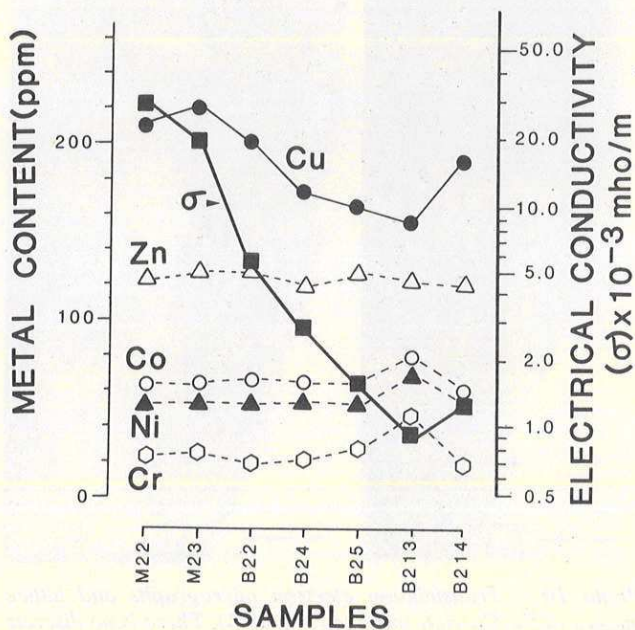


Figure 3 – Electrical conductivity of trace metal contents of basalt samples

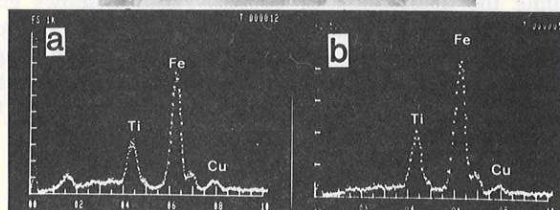
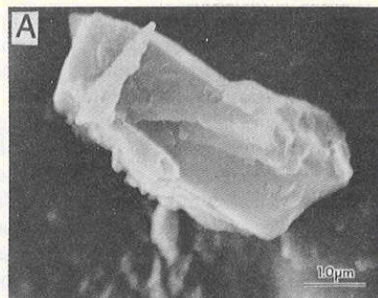


Photo 7 – Scanning electron micrographs of titanomagnetite crystals (A and B) and their EDX (a and b)

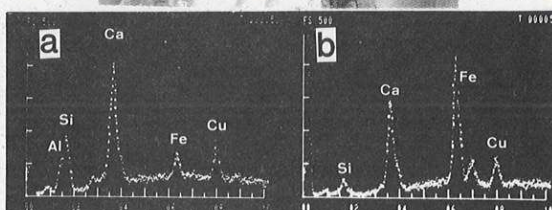
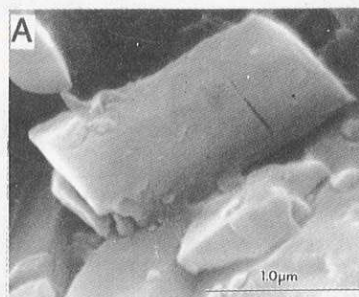


Photo 8 – Scanning electron micrographs of carbonate minerals (A and B) and their EDX (a and b) showing some clay minerals association

Chemical analysis by XRF (Table 1) showed typical basalt composition with a quite normal copper content near 100 ppm. The rather high potassium content is typical of basalts showing some contamination by continental crust.

SIMS analysis of plagioclase, pyroxene and magnetite gave the results shown in figures 1 and 2. The trace elements Zn, Cu, Ni, Co, Cr, and V appear to be most highly concentrated in magnetite. Copper (mass numbers of 63 and 65) was not detected in pyroxene or plagioclase by this method. The rather large SIMS beam size ($\approx 100\mu\text{m}$) can lead to some signals from surrounding materials and the detection of elements such as Li, Be, B, F, Rb, Mo, could suggest the glassy phase.

Electron microprobe analysis of pyroxenes indicated an iron-rich augite. Magnetite analyses showed high Ti contents. No copper was detected in primary phases by EPMA (detection limit $\approx 0.03\%$ Cu).

EPMA back scattered electron images of glassy materials and smectite are shown in photo 3. The smectite derived from glass shows Si, Al, Fe, Ca, and Mg and very small traces of Ti and Cu.

SEM and EDX proved to be the most useful tool for revealing the distribution of copper. Photo 4 shows glass devitrification textures. In some materials, EDX produced a pure copper signal (Photo 4) which implies a native copper film (with the possibility of a copper oxide). It is clear that in this type of material the copper is clearly separated in the

alteration processes, a phenomenon well known in native copper deposits.

In some of the scaly alteration materials (Photo 5), EDX signals showed Fe and Cu contents. These elements appear to be arranged in sheets or films on the surfaces. A remarkable hexagonal form, approximately $1\mu\text{m}$ in width, showed Fe and Cu signals (Photo 6). This crystal appear hollow and filled with smectite. We have not been able to uniquely identify these mixed Fe-Cu phases but they must either be native metals or oxides. These are a wide range of minerals as $\text{Cu}_2\text{O} \cdot \text{Fe}_2\text{O}_3$ (delafossite) and $\text{CuO} \cdot \text{Mn}_2\text{O}_3$ (crednerite) which occur in minor species often associated with clays (Ford 1932).

Some titanomagnetite (Photo 7) contain small amounts of copper and copper is observed with carbonate and clay alteration (Photo 8). Clay formed by glass alteration also appears to be associated with copper (Photo 9). Photo 10 shows high resolution TEM images of alteration products with 10, 11, and 12.5Å spacing of characteristic smectite or mica minerals. These d-spacings were reduced by dehydration from 14-18 Å. No copper was observed in this (001) structure.

Wager & Mitchell (1951) showed that in the Skaergaard, copper concentrations in pyroxenes can reach 1,000 ppm (see also Deer, Howie & Zussman 1962). But copper was not detected in pyroxene by SIMS and electron microscopes in our studies.

Electrical conductivity The copper content for 130 samples of basalts appear to be fresh from the Serra Geral formation varies between 150 and 200 ppm. The drill cores

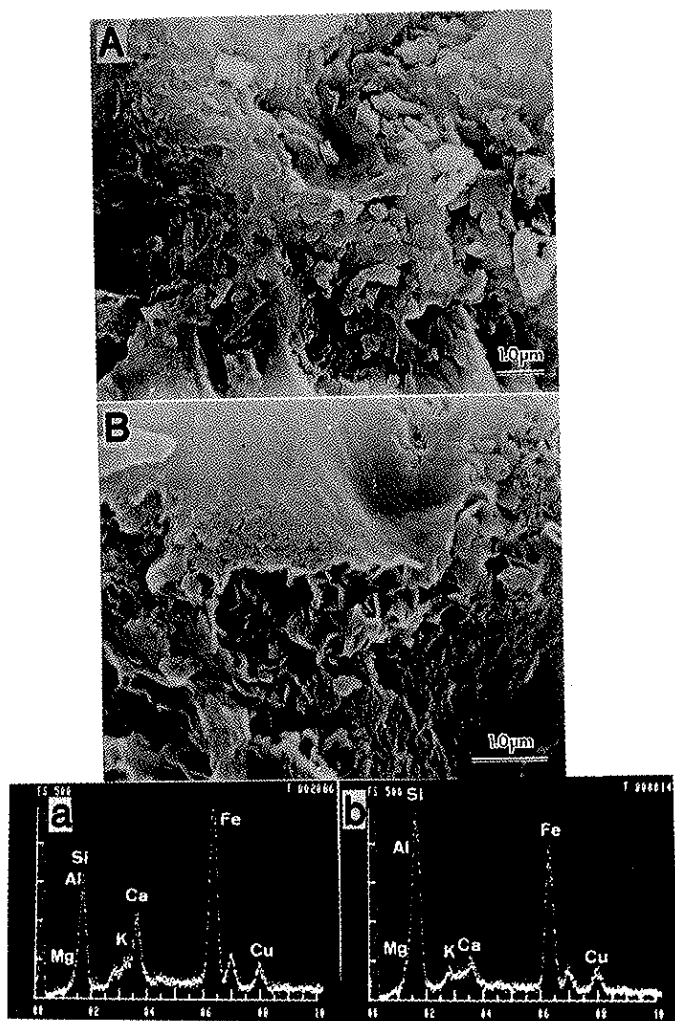


Photo 9 – Scanning electron micrographs of smectite flakes on the surface of devitrification glasses (A and B) and their EDX (a and b)

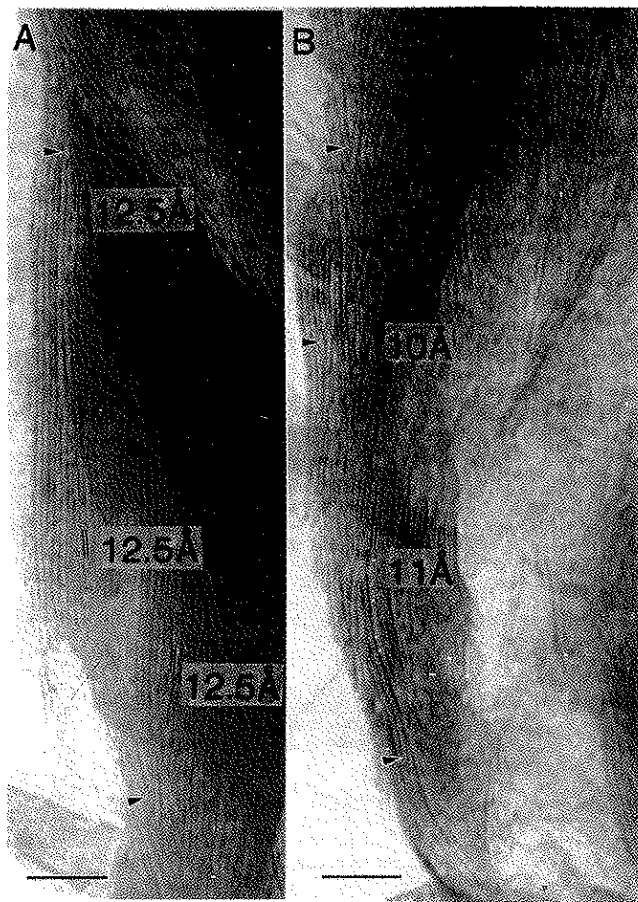


Photo 10 – Transmission electron micrographs and lattice images of Fe-Cu-rich smectite (A and B). There is no discrete copper phase. The arrows indicate dislocations. The scale in A and B indicates 200 Å

were used for measurement of electrical properties of basalts. The measurement of resistivity was carried with the same equipment and method as Telford *et al.* (1976). In general, there is some correlation with electrical conductivity (Fig. 2). Most other trace metals (Fig. 2) show less variation and do not relate to the conductivity (Bischoff & Rocha unpub. data).

We have found evidence for very thin copper films in the alteration zones. The occurrence of native copper as a product of low temperature basalt alteration is common as in the famous Lake Superior deposits of North Michigan. Native copper is found in modern sea floor environments and even in peat swamps (Shotyk unpub. data). As long as circulating warm fluids are low in reduced sulphurs native copper is a favorable product when such fluids are reduced.

Copper appears also to be enriched in the clay-carbonate

alteration products of glass. It is possible that metal-rich swelling clays (smectites) could contribute to conductivity. Copper is known to occur in some clays and is extremely difficult to remove by leaching (Stephens & Metz 1967, Hazen & Wones 1972, Sayin 1982). It is also known that spin exchange between Cu^{2+} and Fe^{3+} can occur over atomic separation of several angstrom (McBride & Mortland 1974).

Copper has been mobile during the low-temperature hydrothermal alteration of the basalts and electrical conductivity patterns may have potencial use in the study of patterns of fluid circulation during cooling. If the high conductivity is indeed caused by thin films of native copper, patterns of basalt conductivity over large areas could suggest the form of water cooling patterns and could show regions where flow has been most pronounced (Fyfe 1985).

REFERENCES

- DEER, W.A.; HOWIE, R.A.; ZUSSMAN, J. 1962. *Rock-forming minerals*. Longmans.
- FORD, W.E. 1932. *A textbook of mineralogy*. New York, John Wiley & Sons, 851 p.
- FYFE, W.S. 1985. Global tectonics and resources. *Comun. Serv. Geol. Portugal*, T. 71, fasc. 1:3-15.
- HAZEN, R.M. & WONES, D.R. 1972. The effect of cation substitutions on the physical properties of trioctahedral mica. *Amer. Mineralogist*, 57:103-129.
- MCBRIDE, M.B. & MORTLAND, M.M. 1974. Copper (II) interactions with montmorillonite: Evidence from physical methods. *Soil Sci. Soc. Amer. Proc.*, 38:408-415.
- PETRI, S. & FULFARO, V.J. 1983. *Geologia do Brasil: Fanerozoico*. São Paulo, Universidade de São Paulo, 631 p.
- SAYIN, M. 1982. Catalytic action of copper on the oxidation of structural iron in vermiculitized biotite. *Clays and Clay Minerals*, 30:287-290.
- STEPHENS, J.D. & METZ, R.A. 1967. The occurrence of copper-bearing clay minerals in oxidized portions of the disseminated copper deposits at Ray, Arizona. *Geol. Soc. Amer. Abs. and Programs*, Ann. Meeting (New Orleans), 213 p.
- TELFORD, W.M.; GELDART, L.P.; SHERIFF, R.E.; KEYS, D.A. 1976. *Applied geophysics*. Cambridge University Press. 444-457.
- WAGER, L.R. & MITCHELL, R.L. 1951. The distribution of trace elements during strong fracturation of basic magma - a further study of the Skaergaard intrusion, East Greenland. *Geochim. Cosmoch. Acta*, 1:129-208.

MANUSCRITO 423

Recebido em 18 de fevereiro de 1987

Revisão aceita em 14 de abril de 1988